Weak Anti-Localization and Quantum Oscillations in Topological Crystalline Insulator PbTe *

Ke-Jie Wang(王克杰), Wei Wang(王伟), Min-Hao Zhang(张敏昊), Xiao-Qian Zhang(张晓倩), Pei Yang(杨沛), Bo Liu(刘波), Ming Gao(高明), Da-Wei Huang(黄大威), Jun-Ran Zhang(张军然), Yu-Jie Liu(刘玉杰), Xue-Feng Wang(王学锋), Feng-Qiu Wang(王枫秋), Liang He(何亮)**, Yong-Bing Xu(徐永兵)**, Rong Zhang(张荣)

Jiangsu Provincial Key Laboratory of Advanced Photonic and Electronic Materials, Jiangsu Provincial Key Laboratory for Nanotechnology, Collaborative Innovation Center of Advanced Microstructures, School of Electronic Science and Engineering, Nanjing University, Nanjing 210093

(Received 11 October 2016)

Topological crystalline insulators (TCIs) have attracted worldwide interest since their theoretical predication and have created exciting opportunities for studying topological quantum physics and for exploring spintronic applications. In this work, we successfully synthesize PbTe nanowires via the chemical vapor deposition method and demonstrate the existence of topological surface states by their 2D weak anti-localization effect and Shubnikov–de Haas oscillations. More importantly, the surface state contributes ∼61% of the total conduction, suggesting dominant surface transport in PbTe nanowires at low temperatures. Our work provides an experimental groundwork for researching TCIs and is a step forward for the applications of PbTe nanowires in spintronic devices.

PACS: 62.23.Hj, 81.07.Gf, 61.46.Km, 05.60.Gg DOI: 10.1088/0256-307X/34/2/026201

Topological crystalline insulators (TCIs) are a recently discovered topological phase with robust surface states residing on high-symmetry crystal surfaces. Different from conventional topological insulators (TIs), protection of the surface states comes from point-group symmetry instead of time-reversal symmetry in TIs.[1–3] The distinct properties of TCIs make them promising candidates for spintronics, quantum computation, tunable pressure sensors, mid-infrared detectors and thermoelectric conversion.[4–7] The exciting discovery and novel properties of TCIs motivate scientists to search the quantum transport phenomenon from the surface states. Theoretical calculations predict that SnTe, PbTe and their related alloy $Pb_{1-x}Sn_xTe$ (Se), possessing high-symmetry rock-salt structure (Fig. 1(a)) with ordered or partially disordered atomic stacking, are stable TCIs. SnTe's surface states with linear Dirac dispersion on mirror-symmetry surfaces have been experimentally detected by angle-resolved photoemission spectroscopy (ARPES),[8,9] and also confirmed through transport measurements.[10–12] In contrast, PbTe's surface states have rarely been observed, mostly due to the shadowing effect from the bulk carrier overwhelming the surface.[13] Thus we have fabricated PbTe nanowires, which possess much higher surface-to-bulk ratio, to probe the topological surface states by transport measurements.

In this work, we report the weak anti-localization (WAL) effect and Shubnikov–de Haas (SdH) oscillations originated from the surface states of PbTe nanowires. We have found that the WAL effect can be well described by the Hikami–Larkin–Nagaoka (HLN) model where the temperature-dependent phase coherent length exhibits a power-law behavior of $l_\Phi \sim T^{-0.47}$.[14] Also, the SdH oscillations reveal a defined 2D surface state in the PbTe nanowire. More importantly, the surface contribution to the total conduction has been estimated as ∼61% at low temperatures, which suggests dominant surface transport in PbTe nanowires.

Following the procedure reported by Tanaka *et al.*,[15] crystal boules of PbTe were produced using a modified Bridgman method. High purity Pb (99.999%) and Te (99.999%) were mixed with an atomic ratio of 1 and were sealed in an evacuated quartz tube. The quartz tube was placed horizontally into a box furnace and heated to 950℃ for two days. After that, the tube was slowly cooled to 770℃ at a rate of 2℃/h and then rapidly cooled down to room temperature. The as-grown PbTe bulk crystal is shown in Fig. 1(b). To check the phase purity, powder x-ray diffraction patterns were obtained, as shown in Fig. 1(c), demonstrating the standard PbTe Bragg peaks. The PbTe nanowires then were synthesized by means of PbTe powder deposited on Si substrates via the chemical vapor deposition (CVD) method with gold catalysts by the vapor–liquid–solid (VLS) mechanism in quartz tube furnace.[16] PbTe powder was loaded in the center of the quartz tube and Au-coated Si substrates were placed at 10–15 cm downstream away from PbTe. The quartz tube was sealed and evacuated. Then high-purity Ar gas was used to flush the quartz tube three times to provide an oxygen-free en-

*Supported by the National Key Research and Development Program of China under Grant No 2016YFA0300803, the National Basic Research Program of China under Grant No 2014CB921101, and the National Natural Science Foundation of China under Grant Nos 61474061 and 61674079.

**Corresponding author. Email: heliang@nju.edu.cn; ybxu@nju.edu.cn.

vironment. After that Ar gas was fed at a constant flow rate of 30 sccm and the tube pressure was maintained at 80 Pa by oil-free scroll pump. In 60 min the furnace and Si substrate temperatures raised up to 880℃ and 560℃, respectively. The growth time was 20 min and then the furnace was cooled down to room temperature.

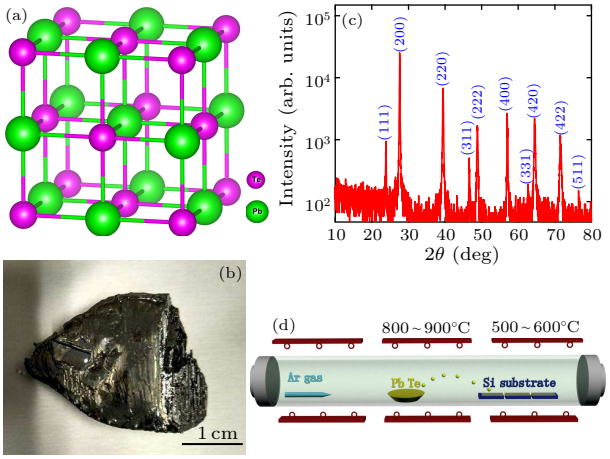

Fig. 1. (a) Schematic view of the cubic structure of PbTe. (b) The image of PbTe bulk material. (c) X-ray diffraction pattern of a crushed PbTe bulk sample. All peaks can be indexed as PbTe's standard Bragg peaks. (d) Schematic drawing of the vapor deposition growth process for PbTe nanowires.

The composition of PbTe nanowires was analyzed by energy-dispersive x-ray spectroscopy (SEM-EDX), as shown in Fig. 2(a), and the estimated atomic ratio of Pb:Te is ∼0.92. Figure 2(b) represents an SEM image of a PbTe nanowire with Au catalysts on the tip. Figures 2(c)–2(e) exhibit the elemental mappings of the tip section, indicated by the white square in Fig. 2(b). It is clearly demonstrated that Pb and Te are uniformly distributed in the nanowire, and Au is only clustered at the tip.

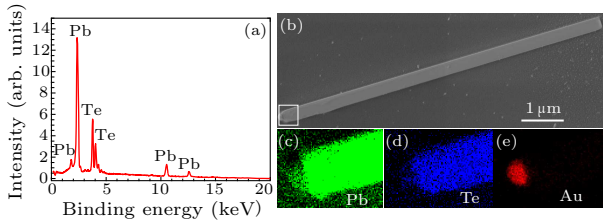

Fig. 2. (a) The SEM-EDX spectrum of a PbTe nanowire exhibiting peaks from Pb and Te only. (b) The SEM image of a PbTe nanowire with a small gold catalyst on the tip. (c)–(e) The elemental mappings of the tip section, indicated by the white square in (b). Pb and Te are evenly distributed in the nanowire, and the Au signal can only be seen on the tip of the nanowire.

To investigate the surface states' transport of PbTe nanowires, four-terminal devices of PbTe nanowires are fabricated, as shown in the inset of Fig. 3(a). As plotted in Fig. 3(a) the temperature-dependent longitudinal resistance exhibits a peak at 80 K. The R–T curves show both semiconductive and metallic features at high temperatures, similar to those reported for 3D topological insulator Bi_2Te_3 nanowires.[17] In the low-temperature region, however, the resistance saturates to a constant value. This is not consistent with any bulk conduction, and has often been observed in surface-state-dominated topological insulators.[18] Thus we believe that this gives us the first hint of the PbTe nanowires' surface states.

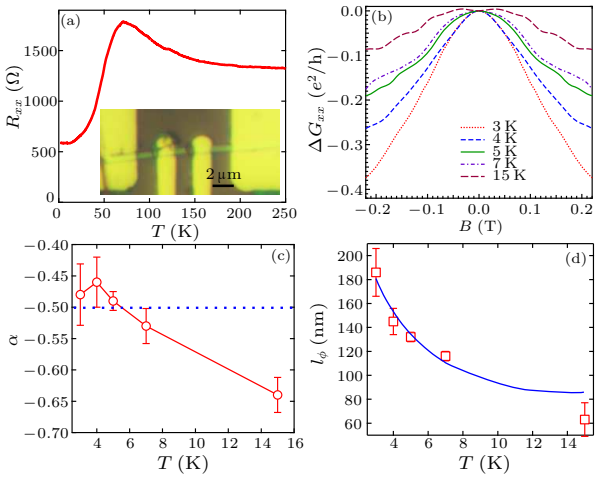

Fig. 3. Magnetotransport of the PbTe nanowire. (a) Temperature-dependent longitudinal resistance R_{xx}. Inset: the microscope image representing the length of the nanowire with gold contact pads. (b) Magnetoconductance in perpendicular magnetic field at 3, 4, 5, 7 and 15 K, indicating the WAL effect. (c) The temperature-dependent α. All of them except $T = 15$ K are near -0.5, indicating that there is only one conducting channel at low temperatures. (d) Temperature dependence of the phase coherent length. The solid (blue) line exhibits the power law dependence as $l_\phi \sim T^{-0.47}$, suggesting that the WAL effect is originated from the 2D surface states for low temperatures (≤7 K).

As a quantum correction to classical magnetoresistance, the WAL effect is a signature of topological surface states originating from Berry's phase. As shown in Fig. 3(b), at low temperatures, the magnetoconductance $\Delta G = G(B) - G(0)$ displays a sharp downward cusp near zero magnetic field, a signature of WAL effect, which is also often observed in the topological insulators.[19–23] With the increase of temperatures, the cusp in the low magnetic field range disappears. This could be attributed to the dramatic decrease of the phase coherence length l_ϕ at high temperature due to the strong thermal scattering.[24] The WAL effect of PbTe nanowire can be described by the HLN model.[25–28] In a strong spin-orbit coupling interaction, i.e., $\tau_\phi \ll \tau_{SO}$ and $\tau_\phi \ll \tau_e$, the conduction correction is given by

$$\begin{aligned}\Delta G_{\rm WAL}(B) &= G(B) - G(0)\\ &= [-(\alpha e^2/2\pi\hbar)][\ln(B_0/B)\\ &\quad - \Psi(1/2 + (B_0/B))],\end{aligned} \tag{1}$$

where $B_0 = \hbar(4\pi l_\phi^2)$ with l_ϕ as the phase coherence length, α is the WAL coefficient, e is the electronic charge, $\hbar$ is the reduced Plank's constant, and Ψ is

the di-gamma function, describing the quantum correction to the conductivity in 2D systems. The $|2\alpha|$ is an estimation of the number of independent channels contributing to the interference.[18,21,23] As shown in Fig. 3(c), the HLN fittings of the low-temperature data ($\leq$7 K) yield $\alpha = -1/2$, suggesting the existence of a single channel, the surface state, consistent with our previous R–T results.[18,26] At 15 K, α deviates from $-1/2$, indicating more conducting channels, possibly from the bulk states. The obtained coherence length decreases from 186 to 62 nm as the temperature increases from 3 to 15 K, as exhibited in Fig. 3(d). Such a dramatic decrease of the coherence length was also observed in other TI systems.[18,27] Theoretically, for a 2D system the temperature-dependent coherence length is described as $l_\Phi \sim T^{-0.5}$, while for 3D systems it is $l_\Phi \sim T^{-0.75}$.[15,22] For temperatures below 7 K, our data yields $l_\Phi \sim T^{-0.47}$ (solid blue line in Fig. 3(d)), indicating that the WAL effect does indeed originate from the 2D surface states at low temperatures. On the contrary, at higher temperatures, the surface state is not the dominant conducting channel anymore, thus α and l_ϕ drift away from the low-temperature data.

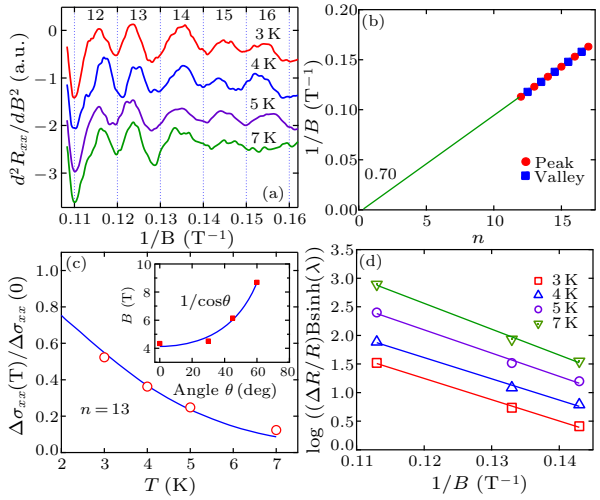

Fig. 4. Shubnikov–de Haas oscillations of the surface states of the PbTe nanowire. (a) The value of d^2R_{xx}/dB^2 versus $1/B$ at various temperatures. Oscillations can be clearly observed. (b) The Landau level fan diagram. Linear fitting gives a nonzero intercept of 0.70$\pm$0.07, suggesting that the Berry Phase is near. (c) Temperature dependence of the normalized conductivity amplitude $\Delta\sigma_{xx}(T)/\Delta\sigma_{xx}(0)$. The solid blue line is fitted by $\lambda(T)/\sinh(\lambda(T))$. The extracted cyclotron mass $m_{\rm cycl}$ is 0.351 m_e. Inset: the magnetic field of landau level $n = 12$ versus the out-of-plane rotation angle. It shows $1/\cos\theta$, suggesting the 2D nature of the Fermi surface. (d) Dingle plot of $\log[(\Delta R/R)B\sinh(\lambda)]$ versus $1/B$ at different temperatures. Transport lifetime τ can be extracted from the fitting of $\log[(\Delta R/R)B\sinh(\lambda)]$.

As a powerful tool, the SdH oscillations have been widely used to explore the surface states in high quality topological insulators.[28–31] In Fig. 4(a), the oscillatory part of d^2R_{xx}/dB^2 displays periodic peaks (minima) and valleys (maxima) with $1/B$, indicating the existence of a well-defined Fermi surface up to 7 K.[31] For a 2D Fermi surface, the peak positions depend only on the perpendicular field $B_\perp = B\cos\theta$ along the axis z, and θ is the tilt angle between z and B. As shown in the inset of Fig. 4(c), the dependence of Landau level $n = 12$ on rotation angle matches perfectly with $1/\cos\theta$, indicating the 2D nature of the SdH oscillations. Moreover, the SdH oscillation frequency has a direct relationship with the Fermi surface $S_{\rm F}$ via the Onsager relation: $f_{\rm SDH} = (h/4\pi^2 e)S_{\rm F}$. Thus we can deduce the Fermi vector $k_{\rm F} = \sqrt{(S_{\rm F}/\pi)} = 5.5\times10^6\,{\rm cm}^{-1}$ and the 2D carrier density $n_{\rm 2D} = k_{\rm F}^2/4\pi = 2.4\times10^{12}\,{\rm cm}^{-2}$.

We have also plotted the Landau level fan diagram in Fig. 4(b). The maxima and the minima in Fig. 4(a) are represented by red circles and blue squares, respectively. Very good linear fitting gives the horizontal axis intercept of 0.70 $\pm$ 0.07. The value is close to 1/2, indicating the existence of the Berry phase π, highlighting that the SdH oscillations originate from the 2D topological surface states.[32–34] To obtain the cyclotron mass ($m_{\rm cycl}$), we have fitted the temperature-dependent amplitude of $\Delta\sigma_{xx}(T)/\Delta\sigma_{xx}(0) = \lambda(T)/\sinh(\lambda(T))$, where $\lambda(T) = 2\pi^2 K_{\rm B}Tm_{\rm cycl}/\hbar eB$. As shown in Fig. 3(c), the best fitting gives $m_{\rm cycl} = 0.351m_{\rm e}$ at $B = 7.8$ T. The cyclotron mass and Fermi velocity satisfy $m_{\rm cycl}\nu_{\rm F} = \hbar k_{\rm F}$,[35] thus $\nu_{\rm F}$ can be estimated to be $1.82\times10^5\,{\rm ms}^{-1}$, which in turn gives the Fermi level $E_{\rm F} = m_{\rm cycl}\nu_{\rm F}^2 = 66$ meV.[35] The transport lifetime τ can be deduced from the slope of Dingle plot by $\log[(\Delta R/R)B\sinh(\lambda(T))]$,[32,36] where $\Delta R/R \sim [\lambda(T)/\sinh\lambda(T)]e^{-D}$ and $D = 2\pi^2 E_{\rm F}/\tau eB\nu_{\rm F}^2$. As shown in Fig. 4(d), the fitting gives $\tau = 1.05\times10^{-12}$ s and the corresponding mean free path $l = \nu_{\rm F}\tau = 194$ nm, similar to the previous calculated phase coherent length l_ϕ (~186 nm). The surface electrons' mobility $\mu_{\rm s} = e\tau/m_{\rm cycl} = el/\hbar k_{\rm F}$=5335 ${\rm cm}^2{\rm V}^{-1}{\rm s}^{-1}$. Such high mobility confirms that the conducting carriers come from the surface states. According to the calculated results, the surface contribution to the total conduction can be estimated as ~61%,[22] further demonstrating that the low-temperature conductance is mainly from the surface states, as the SdH oscillations.

In summary, we have synthesized high-quality single crystalline PbTe nanowires via CVD using Au catalysts, from which quantum oscillations and the WAL effect from the topological surface states have been observed. More importantly, the surface state contributes up to ~61% of the total conduction at low temperatures. The discovery of surface Dirac electrons in PbTe nanowires is one step forward to their applications in spintronic and nanoelectronics.

References

[1] Fu L 2011 *Phys. Rev. Lett.* **106** 106802

[2] Bernevig B A, Hughes T L and Zhang S C 2006 *Science* **314** 1757
[3] Bernevig B A and Zhang S C 2006 *Phys. Rev. Lett.* **96** 106802
[4] Wang Q, Wang F, Li J, Wang Z, Zhan X and He J 2015 *Small* **11** 4613
[5] Fu L and Kane C L 2008 *Phys. Rev. Lett.* **100** 096407
[6] Wang Q, Safdar M, Wang Z and He J 2013 *Adv. Mater.* **25** 3915
[7] Kong D and Cui Y 2011 *Nat. Chem.* **3** 845
[8] Dziawa P, Kowalski B J, Dybko K, Buczko R, Szczerbakow A, Szot M, Lusakowska E, Balasubramanian T, Wojek B M, Berntsen M H, Tjernberg O and Story T 2012 *Nat. Mater.* **11** 1023
[9] Xu S Y, Liu C, Alidoust N, Neupane M, Qian D, Belopolski I, Denlinger J D, Wang Y J, Lin H, Wray L A, Landolt G, Slomski B, Dil J H, Marcinkova A, Morosan E, Gibson Q, Sankar R, Chou F C, Cava R J, Bansil A and Hasan M Z 2012 *Nat. Commun.* **3** 1192
[10] Safdar M, Wang Q, Mirza M, Wang Z, Xu K and He J 2013 *Nano Lett.* **13** 5344
[11] Li Z, Shao S, Li N, McCall K, Wang J and Zhang S X 2013 *Nano Lett.* **13** 5443
[12] Kong D, Dang W, Cha J J, Li H, Meister S, Peng H, Liu Z and Cui Y 2010 *Nano Lett.* **10** 2245
[13] Peng H, Lai K, Kong D, Meister S, Chen Y, Qi X L, Zhang S C, Shen Z X and Cui Y 2010 *Nat. Mater.* **9** 225
[14] Altshuler B L, Aronov A G and Khmelnitsky D E 1982 *J. Phys.* C **15** 7367
[15] Tanaka Y, Ren Z, Sato T et al 2012 *Nat. Phys.* **8** 800
[16] Tanaka Y, Sato T, Nakayama K, Souma S, Takahashi T, Ren Z, Novak M, Segawa K and Ando Y 2013 *Phys. Rev.* B **87** 155105
[17] Kong D, Randel J C, Peng H, Cha J J, Meister S, Lai K, Chen Y, Shen Z X, Manoharan H C and Cui Y 2010 *Nano Lett.* **10** 329
[18] Cha J J, Kong D, Hong S S, Analytis J G, Lai K and Cui Y 2012 *Nano Lett.* **12** 1107
[19] He L, Xiu F X, Wang Y, Fedorov A V, Huang G, Kou X F, Lang M, Beyermann W P, Zou J and Wang K L 2011 *J. Appl. Phys.* **109** 103702
[20] Zhang C, Liu Y, Yuan X, Wang W, Liang S and Xiu F 2015 *Nano Lett.* **15** 2161
[21] Bao L H, He L, Meyer N, Kou X F, Zhang P, Chen Z G, Fedorov A V, Zou J, Riedemann T M and Lograsso T A 2012 *Sci. Rep.* **2** 726
[22] He H T, Wang G, Zhang T, Sou I K, Wong G K, Wang J N, Lu H Z, Shen S Q and Zhang F C 2011 *Phys. Rev. Lett.* **106** 166805
[23] van Hove J M, Pukite P R and Cohen P I 1985 *J. Vac. Sci. Technol.* B **3** 563
[24] Hikami S, Larkin A I and Nagaoka Y 1980 *Prog. Theor. Phys.* **63** 707
[25] Chen J, Qin H J, Yang F, Liu J, Guan T, Qu F M, Zhang G H, Shi J R, Xie X C, Yang C L, Wu K H, Li Y Q and Lu L 2010 *Phys. Rev. Lett.* **105** 176602
[26] Matsuo S, Koyama T, Shimamura K, Arakawa T, Nishihara Y, Chiba D, Kobayashi K, Ono T, Chang C, He K, Ma X C and Xue Q K 2012 *Phys. Rev.* B **85** 075440
[27] Analytis J G, McDonald R D, Riggs S C, Chu J, Boebinger G S and Fisher I R 2010 *Nat. Phys.* **6** 960
[28] Ohta E and Sakata M 1979 *Solid-State Electron.* **22** 677
[29] Taskin A A and Ando Y 2009 *Phys. Rev.* B **80** 085303
[30] Xiu F, He L, Wang Y, Cheng L, Chang L T, Lang M, Huang G, Kou X, Zhou Y, Jiang X, Chen Z, Zou J, Shailos A and Wang K L 2011 *Nat. Nanotechnol.* **6** 216
[31] Eto K, Ren Z, Taskin A A, Segawa K and Ando Y 2010 *Phys. Rev.* B **81** 195309
[32] Taskin A A, Yang F, Sasaki S, Segawa K and Yoichi A 2014 *Phys. Rev.* B **89** 121302
[33] Qu D X, Hor Y S, Xiong J, Cava R J and Ong N P 2010 *Science* **329** 821
[34] Fang L, Jia Y, Miller D J, Latimer M L, Xiao Z L, Welp U, Crabtree G W and Kwok W K 2012 *Nano Lett.* **12** 6164
[35] Hong S S, Cha J J, Kong D and Cui Y 2012 *Nat. Commun.* **3** 757
[36] Analytis J G, Chu J, Chen Y L, Corredor F, McDonald R D, Shen Z X and Fisher I R 2010 *Phys. Rev.* B **81** 205407